Intermittency of quasi-static magnetohydrodynamic turbulence: A wavelet viewpoint

Naoya Okamoto[1], Katsunori Yoshimatsu[2], Kai Schneider[3] and Marie Farge[4]

[1]Center for Computational Science, Nagoya University, Japan,
[2]Department of Computational Science and Engineering, Nagoya University, Japan,
[3]M2P2–CNRS and Universités d'Aix-Marseille, France,
[4]LMD–IPSL–CNRS, Ecole Normale Supérieure, France

E-mail: okamoto@ccs.engg.nagoya-u.ac.jp

Abstract. Intermittency of quasi-static magnetohydrodynamic (MHD) turbulence in an imposed magnetic field is examined, using three-dimensional orthonormal wavelets. The wavelet analysis is applied to two turbulent MHD flows computed by direct numerical simulation with 512^3 grid points and with different intensities of the imposed magnetic field. It is found that the imposed magnetic field leads to a substantial amplification of intermittency of the flow, especially in the direction of the imposed magnetic field.

1. Introduction

Quasi-static magnetohydrodynamic (MHD) turbulence subject to an imposed magnetic field exhibits multiscale anisotropy and spatial intermittency. Different tools to quantify the anisotropy of turbulence have been developed so far (see e.g., Knaepen & Moreau, 2008). Spectral analyses, while capturing the multiscale character, cannot quantify the spatial intermittency of the flows. However, the wavelet representation can simultaneously examine information on space, scale and direction, since the representation is based on functions localized in space, scale and direction. Wavelet techniques have been used to analyze, model and compute turbulent flows. Readers interested in applications of wavelet techniques to fluid dynamics may refer to the recent review articles (Farge, 1992; Schneider & Vasilyev, 2010). In this paper we study the influence of the strength of the magnetic field on the intermittency and the anisotropy of quasi-static MHD turbulence, using wavelet-based statistics introduced in Bos *et al.* (2007). Further details of the study can be found in Okamoto *et al.* (2011).

2. Direct numerical simulation of quasi-static MHD turbulence

We consider homogeneous MHD turbulence of incompressible fluid in a uniform magnetic field $\boldsymbol{B}_0$ in a 2π periodic box. In the limit of low magnetic Reynolds number, the motion of the flow obeys the following equations under the so-called quasi-static MHD approximation (see e.g.,

Knaepen *et al.*, 2004),

$$\frac{\partial}{\partial t}\boldsymbol{u} + (\boldsymbol{u}\cdot\nabla)\boldsymbol{u} = -\frac{1}{\rho}\nabla p + \nu\Delta\boldsymbol{u} - \frac{\sigma}{\rho}\Delta^{-1}(\boldsymbol{B}_0\cdot\nabla)^2\boldsymbol{u} + \boldsymbol{f}, \tag{1}$$

$$\nabla\cdot\boldsymbol{u} = 0. \tag{2}$$

Here, $\boldsymbol{u}$ is the velocity field, ρ the fluid density, ν the kinematic viscosity and σ the electrical conductivity. The term $\boldsymbol{f}$ expresses the solenoidal external force applied to the velocity field. The constant magnetic field is given by $\boldsymbol{B}_0 = (0, 0, B_0)$ in the Cartesian coordinate system.

The third term on the right-hand side of equation (1) is the rotational part of the Lorentz force, and the modified pressure p includes both the fluid pressure and the magnetic pressure. The symbol Δ^{-1} represents the inverse Laplace operator. An estimate of the ratio of the Lorentz force to the nonlinear term in equation (1) is given by the interaction parameter $N = \sigma B_0^2 L/(\rho u')$, where $u' = \langle|\boldsymbol{u}|^2\rangle/3$ and L is the integral length scale defined by $L = \pi/(2u'^2)\int E(k)/k\,dk$. Here, $\langle\cdot\rangle$ denotes the spatial average and $E(k)$ is the energy spectrum.

We performed DNS computations at two interaction parameters $N = 1$ and 3. We used a Fourier pseudo-spectral method at 512^3 grid points with a fourth-order Runge-Kutta method for time marching. The external solenoidal random force $\boldsymbol{f}$ is applied to the velocity field only in the low wavenumber range for $k < 2.5$.

3. Wavelet-based statistics

The velocity field $\boldsymbol{u} = (u^1, u^2, u^3)$, sampled at resolution $n = 2^{3J}$, is decomposed into an orthogonal discrete wavelet series,

$$\boldsymbol{u}(\boldsymbol{x}) = \sum_{\lambda} \widetilde{\boldsymbol{u}}_\lambda \psi_\lambda(\boldsymbol{x}), \tag{3}$$

where the multi-index $\lambda = (j, \boldsymbol{i}, d)$ denotes, for each wavelet ψ_λ, the scale index j (varying from 0 to $J-1$), the spatial index $\boldsymbol{i} = (i^1, i^2, i^3)$, having 2^{3j} values for each j and d, and the direction index $d = 1, ..., 7$. $\boldsymbol{x} = (x^1, x^2, x^3)$. The discrete wavelet basis $\psi_\lambda(\boldsymbol{x})$ consists of continuous functions, although the index set Λ is discrete. The three-dimensional wavelets $\psi_\lambda(\boldsymbol{x})$ correspond to products of one-dimensional scaling functions and wavelets in various combinations, as shown in (Mallat, 2010; Meyer, 1992) and (Meneveau, 1991) for two- and three-dimensional wavelets, respectively. The spatial average of $\psi_\lambda(\boldsymbol{x})$, denoted by $\langle\psi_\lambda(\boldsymbol{x})\rangle$, as well as higher order moments vanish. In the present work, the compactly supported Coiflet wavelets with filter width 12 and 4 vanishing moments are used.

The wavelet coefficients measure the fluctuations of $\boldsymbol{u}$ at scale 2^{-j} and around position $\boldsymbol{i}/2^j$ for each of the seven directions d. The contribution of $\boldsymbol{u}$ at scale 2^{-j} and in direction d, denoted by $\boldsymbol{u}_{j,d}$, is obtained by fixing (j, d) and summing only over $\boldsymbol{i}$ in Eq. (3). By construction we have

$$\boldsymbol{u}(\boldsymbol{x}) = \sum_{j=0}^{J-1}\sum_{d=1}^{7} \boldsymbol{u}_{j,d}(\boldsymbol{x}). \tag{4}$$

Relating scale 2^{-j} with wavenumber k_j as $k_j = k_\psi 2^j$, where k_ψ is the centroid wavenumber of the chosen wavelet, the following wavelet-based statistics were introduced in (Bos *et al.*, 2007). We define the directional wavelet energy spectrum for the velocity component u^ℓ by

$$\widetilde{E}^\ell(k_j, d) = \frac{\langle\{u^\ell_{j,d}(\boldsymbol{x})\}^2\rangle}{2\Delta k_j}, \tag{5}$$

where $\Delta k_j = k_j \ln 2$. Summing $\widetilde{E}^\ell(k_j, d)$ from $d = 1$ to 7 yields the spectrum $\widetilde{E}^\ell(k_j) = \sum_{d=1}^{7} \widetilde{E}^\ell(k_j, d)$. To study higher order statistics, we define the flatness of u^ℓ at scale 2^{-j} and direction d by

$$F_{j,d}^\ell = \frac{\left\langle \{u_{j,d}^\ell(\boldsymbol{x})\}^4 \right\rangle}{\left\langle \{u_{j,d}^\ell(\boldsymbol{x})\}^2 \right\rangle^2}, \tag{6}$$

noting that $\langle u_{j,d}^\ell(\boldsymbol{x}) \rangle = 0$.

The wavelet analysis is applied to the DNS fields at two interaction parameters $N = 1$ and 3. The fields are axisymmetric with respect to the x^3-axis, which is parallel to the imposed magnetic field $\boldsymbol{B}_0$. Hence, we consider the directional statistics only for three principle directions, *i.e.*, $d = 1, 2$ and 3.

4. Numerical Results

To obtain an intuitive idea on the flow structures at $N = 1$ and 3, we visualize the modulus of the vorticity field $|\boldsymbol{\omega}|$ in Figure 1. For $N = 3$, in Figure 1(left), one can see sheet-like structures and tube-like structures. Many of the structures are aligned parallel with the imposed magnetic field $\boldsymbol{B}_0$. The alignment of the structures shows the strong anisotropy of the flow. In contrast, the structures at $N = 1$ in Figure 1 (right) exhibit entangled vortex tubes, which do not seem to be aligned with any specific direction. Thus, the field at $N = 1$ is less anisotropic than that at $N = 3$.

To examine the directional anisotropy of the velocity component u^1 which is perpendicular to $\boldsymbol{B}_0$, we plot directional wavelet energy spectra $\widetilde{E}^1(k_j, d)$ in Fig. 2. For $N = 3$, the largest energy contribution in $\widetilde{E}^1(k_j)$ is made by $\widetilde{E}^1(k_j, 2)$, followed by the remaining spectra, $\widetilde{E}^1(k_j, 1)$ and $\widetilde{E}^1(k_j, 3)$. The statistics for the field at $N = 1$ confirm the weaker anisotropy compared to the

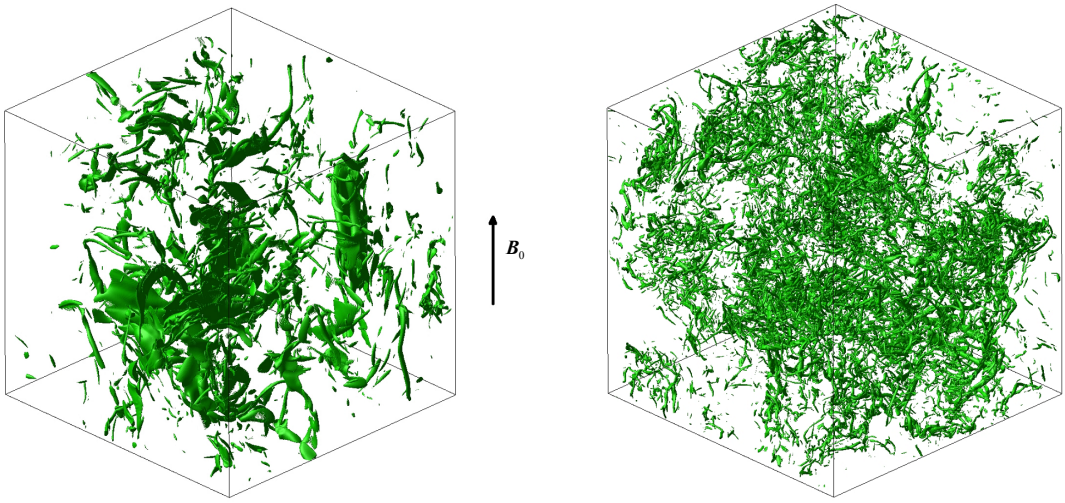

Figure 1. Visualization of intense vorticity regions of the DNS fields for $N = 3$ (left) and $N = 1$ (right) at $t = 9T$. Isosurfaces of $|\boldsymbol{\omega}| = \langle |\boldsymbol{\omega}| \rangle + 4\sigma$ are shown, where σ denotes the standard deviation of $|\boldsymbol{\omega}|$. The vertical arrow indicates the direction of the imposed magnetic field.

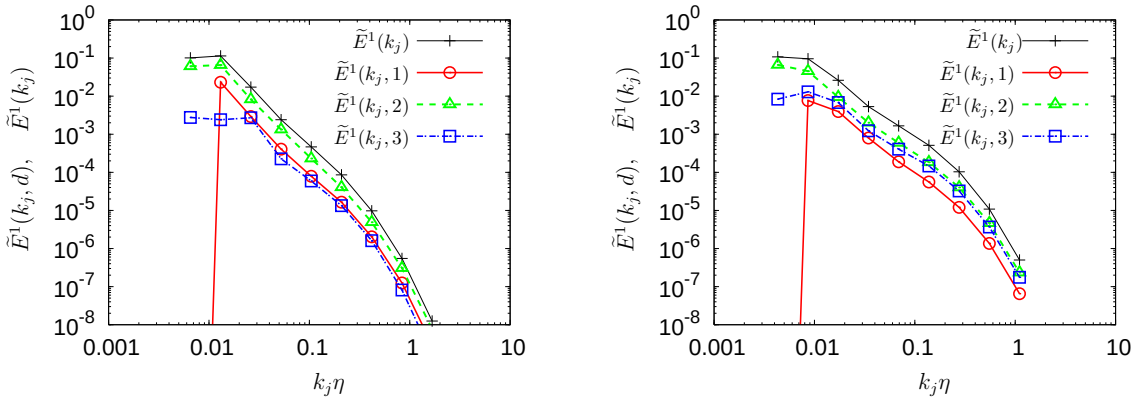

Figure 2. Directional wavelet energy spectra $\widetilde{E}^1(k_j,d)$ vs. $k_j\eta$ for the DNS field with $N=3$ (left), the DNS field with $N=1$ (right), where η is the Kolmogorov dissipation scale. The solid black lines with + show the corresponding wavelet energy spectra $\widetilde{E}^1(k_j)$.

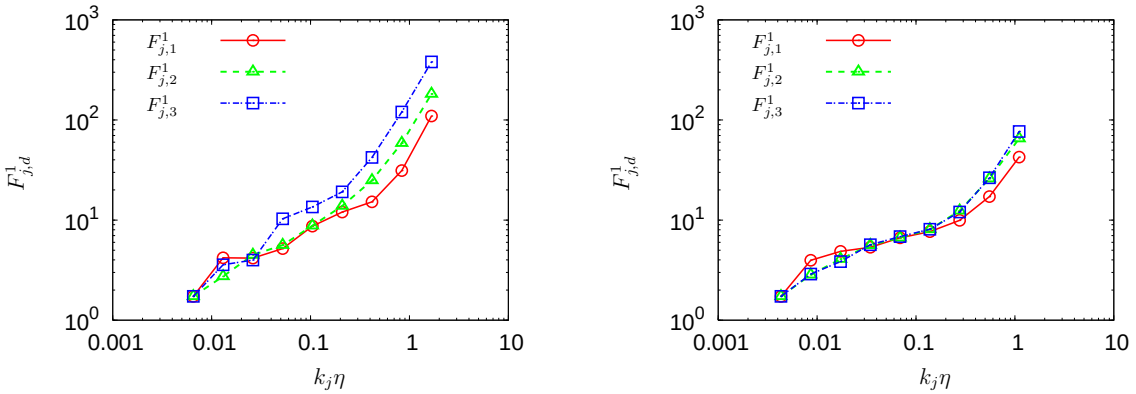

Figure 3. Scale-dependent flatness F^1_j vs. $k_j\eta$ for the DNS fields with $N=1$ (left) and $N=3$ (right).

case $N=3$. The spectra show that $\widetilde{E}^1(k_j,2)\sim\widetilde{E}^1(k_j,3)$ for $k_j\eta\gtrsim 0.03$, while the contribution of $\widetilde{E}^1(k_j,1)$ is smaller.

To get insight into the anisotropy of intermittency, we plot in Fig. 3 the directional scale-dependent flatness $F^1_{j,d}$, $(d=1,2,3)$. For $N=3$ we find that $F^1_{j,3}>F^1_{j,1}$ and $F^1_{j,3}>F^1_{j,2}$ at each scale satisfying $k_j\eta\gtrsim 0.3$. For $N=3$, the flatness values $F^1_{j,d}(d=1,2,3)$ are larger than those for $N=1$. In particular, the flatness in the x^3-direction, $F^1_{j,3}$, for the case $N=3$ is significantly larger than that for $N=1$. These results for the flatness $F^1_{j,d}$ show that the imposed magnetic field $\boldsymbol{B}_0$ plays a significant role on the amplification of small-scale intermittency, especially the intermittency in the x^3-direction, which is parallel to $\boldsymbol{B}_0$.

5. Conclusion and discussion

Our results have shown that the imposed magnetic field $\boldsymbol{B}_0$ plays a significant role, not only for the anisotropy, but also for the amplification of small-scale intermittency, especially in the direction parallel to $\boldsymbol{B}_0$. This is in contrast to the case of incompressible rotating hydrodynamic (HD) turbulence. The rotational effect does not play a major role on the amplification of small-scale intermittency Bos *et al.* (2007). Nevertheless, both rotational HD turbulence and quasi-static MHD turbulence show structures which are aligned with the rotational axis and the imposed magnetic field, respectively.

Acknowledgments

The computations were carried out on the Earth Simulator and the FX1 system at the Information Technology Center of Nagoya University. K.Y. and N.O. are finantially supported by Grant-in-Aids for Young Scientists (B) 22740255 and 22760063, respectively, from the Ministry of Education, Culture, Sports, Science and Technology. M.F. and K.S. thankfully acknowledge financial support from the PEPS program of INSMI-CNRS and also thank the Association CEA-EURATOM and the FRF2S (French Research Federation for Fusion Studies) for supporting their work within the framework of the EFDA (European Fusion Development Agreement) under contract V.3258.001. We acknowledge the CIRM, Luminy, for hospitality during the 2010 CEMRACS summer program on "Numerical modelling of fusion".

References

Bos, W., Liechtenstein, L. & Schneider, K. 2007 Small scale intermittency in anisotropic turbulence. *Phys. Rev.* E **76**, 046310.

Farge, M. 1992 Wavelet transforms and their applications to turbulence. *Annu. Rev. Fluid Mech.* **24**, 395–457.

Knaepen, B., Kassinos, S. & Carati, D. 2004 Magnetohydrodynamic turbulence at moderate magnetic Reynolds number. *J. Fluid Mech.* **513**, 199–220.

Knaepen, B. & Moreau, R. 2008 Magnetohydrodynamic turbulence at low magnetic Reynolds number. *Annu. Rev. Fluid Mech.* **40**, 25–45.

Mallat, S. 2010 *A Wavelet Tour of Signal Processing, Third Edition: The Sparse Way* Academic Press.

Meneveau, C. 1991 Analysis of turbulence in the orthonormal wavelet representation. *J. Fluid Mech.* **232**, 469–520.

Meyer, Y. 1992 *Wavelets and operators, Cambridge Studies in Advanced Mathematics* Cambridge University Press.

Okamoto, N., Yoshimatsu, K., Schneider, K. & Farge, M. 2011 Directional and scale-dependent statistics of quasi-static magnetohydrodynamic turbulence. *ESAIM: Proceedings* (accepted).

Schneider, K. & Vasilyev, O. 2010 Wavelet methods in computational fluid dynamics. *Annu. Rev. Fluid Mech.* **42**, 473–503.